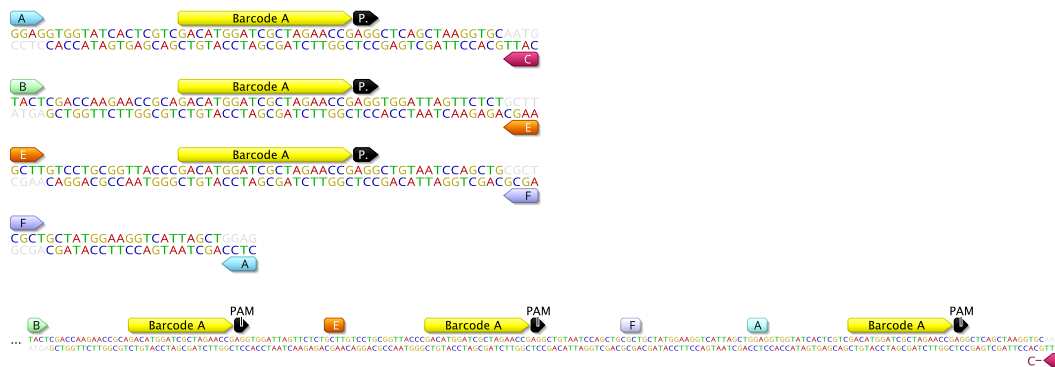


## SUPPLEMENTARY INFORMATION

### Technical Note: Control of lineage-specific gene expression by functionalized gRNA barcodes

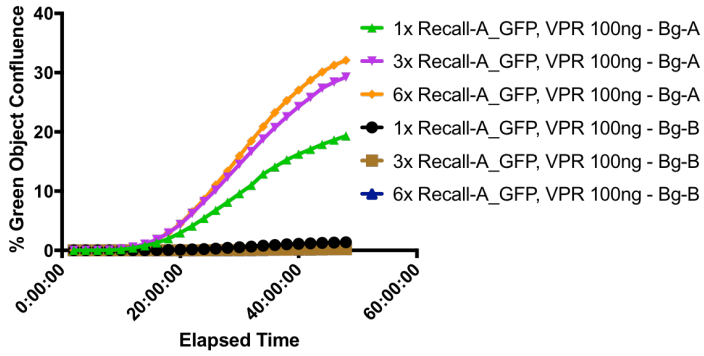
#### 3x Bg-A landing pad array assembly



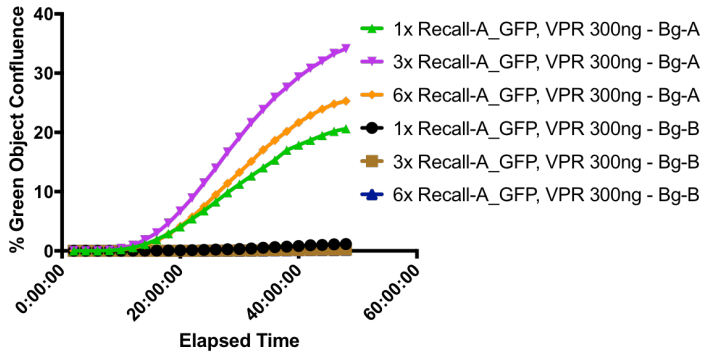
**Supplementary Figure S1. Bg-A landing pad array assembly.** The 3x barcode landing pad arrays were assembled by first annealing complimentary oligonucleotides containing the barcode of interests and PAM site along with the specified overhangs A-F (a). When combined, these specified overhangs drive assembly of the individual double stranded barcodes to both make the 3x barcode array as well as direct integration into the BbsI digested Recall plasmid (b). Similar schemes were used to assemble larger barcode arrays.

## Supplementary Figure S2

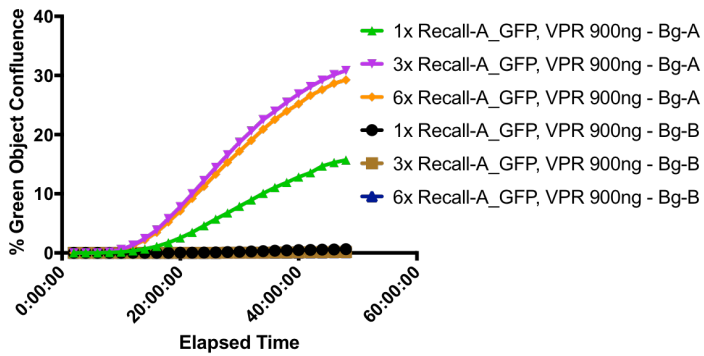
### Barcode A 1/3/6x Array with 100ng dCas9-VPR



### Barcode A 1/3/6x Array with 300ng dCas9-VPR



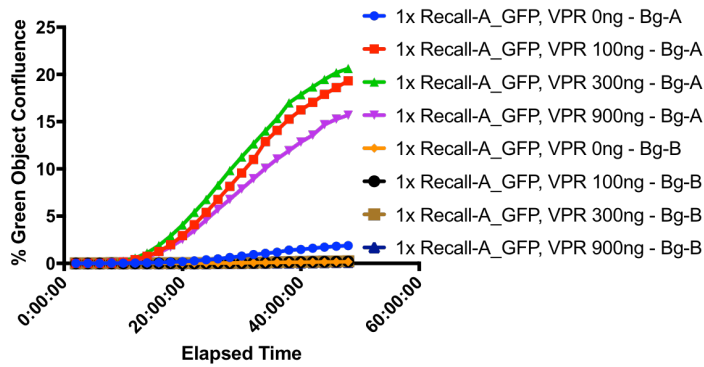
### Barcode A 1/3/6x Array with 900ng dCas9-VPR



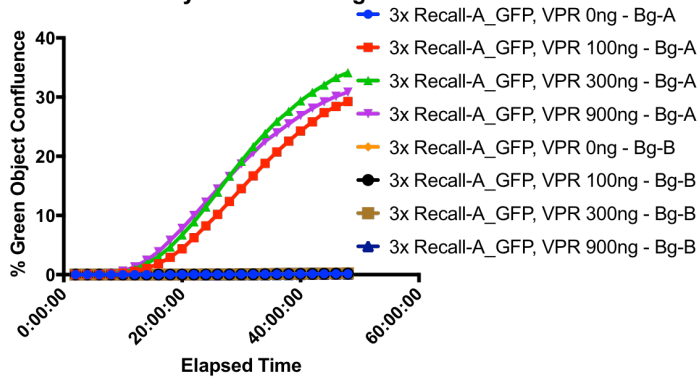
**Supplementary Figure S2. Lineage specific gene activation efficiency of 1x, 3x, 6x barcode landing pads at different concentrations of dCas9-VPR.** Time lapse fluorescent analysis of percent green object confluence of HEK293Ts Bg-A and Bg-B populations co-transfected with dCas9-VPR and 80ng of Recall-A\_GFP plasmids with a 1x, 3x, or 6x barcode array in a 24 well plate. These graphs compare recall activation efficiency between Recall-A\_GFP plasmids with a 1x, 3x, or 6x barcode array at given dCas9-VPR amounts.

## Supplement Figure S3

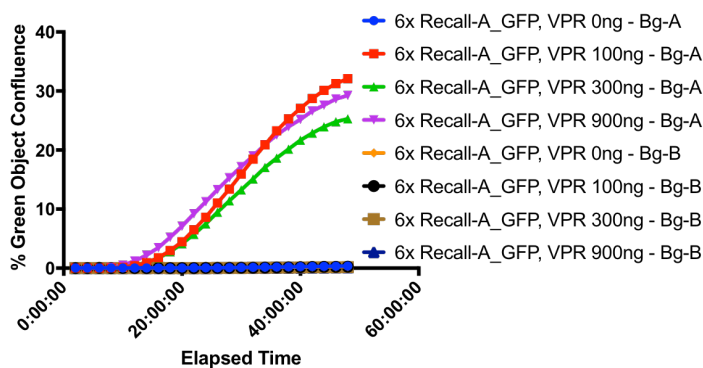
### Barcode A 1x Array with Increasing dCas9-VPR



### Barcode A 3x Array with Increasing dCas9-VPR

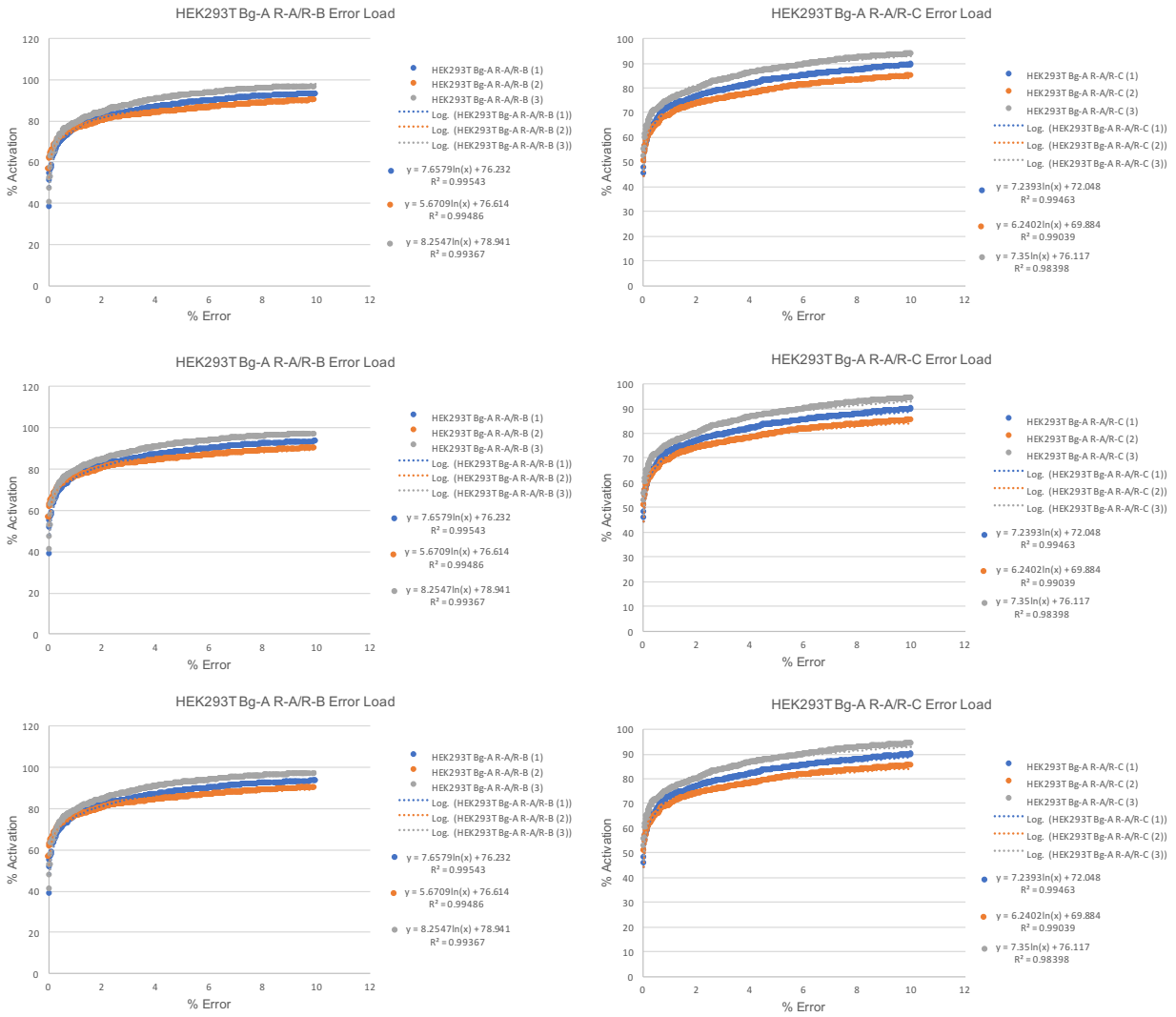


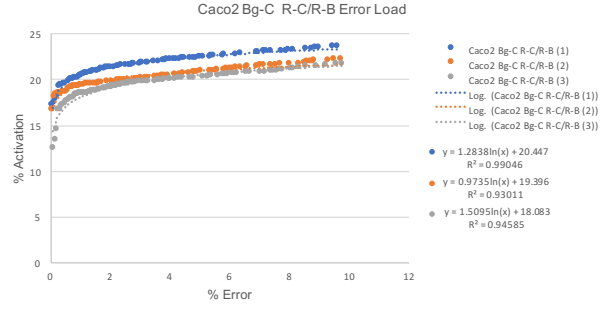
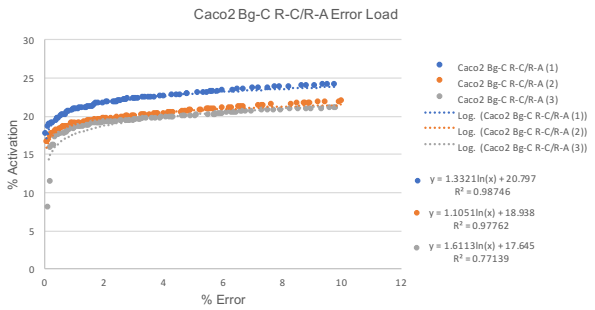
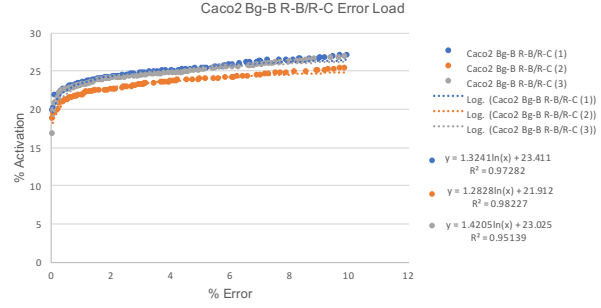
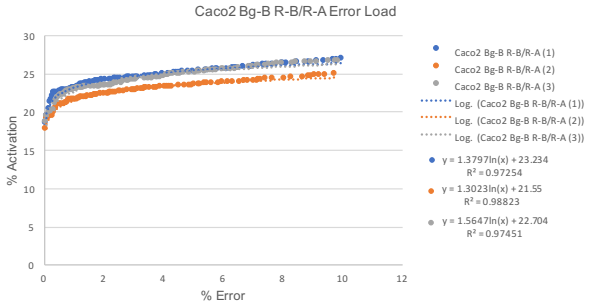
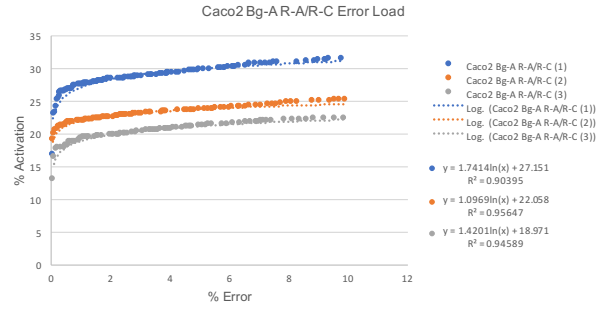
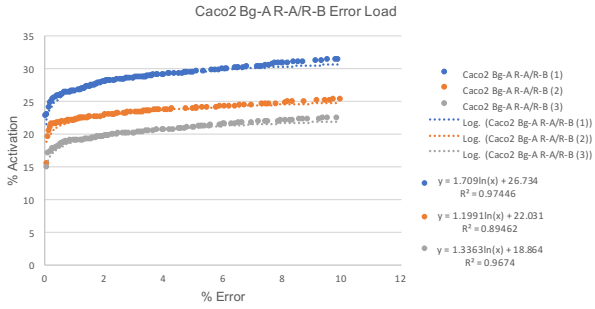
### Barcode A 6x Array with Increasing dCas9-VPR

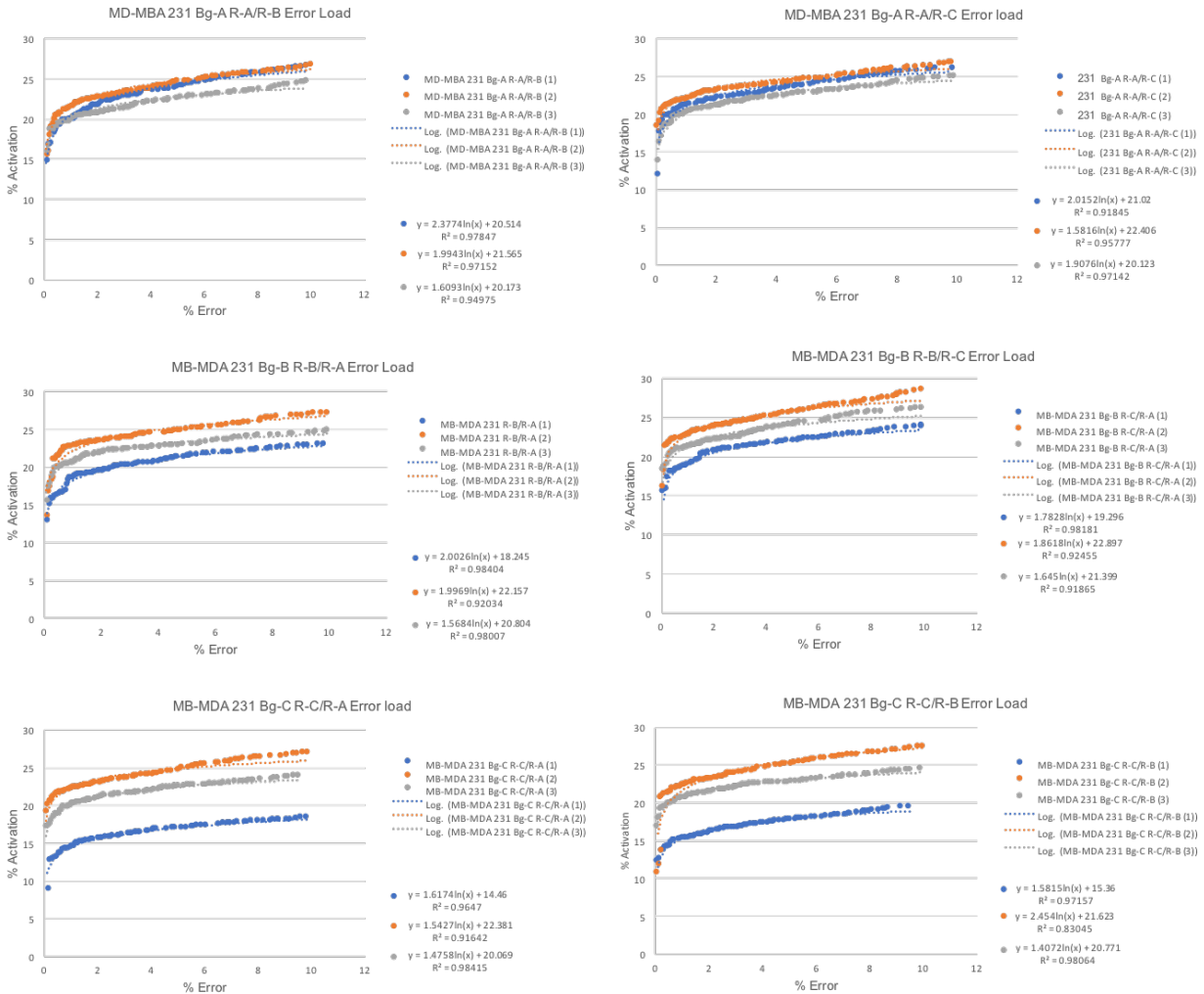


**Supplementary Figure S3. Lineage specific gene activation efficiency with increase concentrations of dCas9-VPR in coordination with 1x, 3x, or 6x barcode landing pads.** Time lapse fluorescent analysis of percent green object confluence of HEK293Ts Bg-A and Bg-B populations co-transfected with 0, 100, 300, and 900ng of dCas9-VPR and 80ng of Recall-A\_GFP plasmids with a 1x, 3x, or 6x barcode array in a 24 well plate. These graphs compare recall activation efficiency of increasing amounts dCas9-VPR when co-transfected with 80ng Recall-A\_GFP plasmids with a 1x, 3x, or 6x barcode array.

# Supplement Figure S4







### Supplementary Figure S4. Error load quantification.

Independent barcoded populations, Bg-A, Bg-B, and Bg-C, were generated in cell lines:

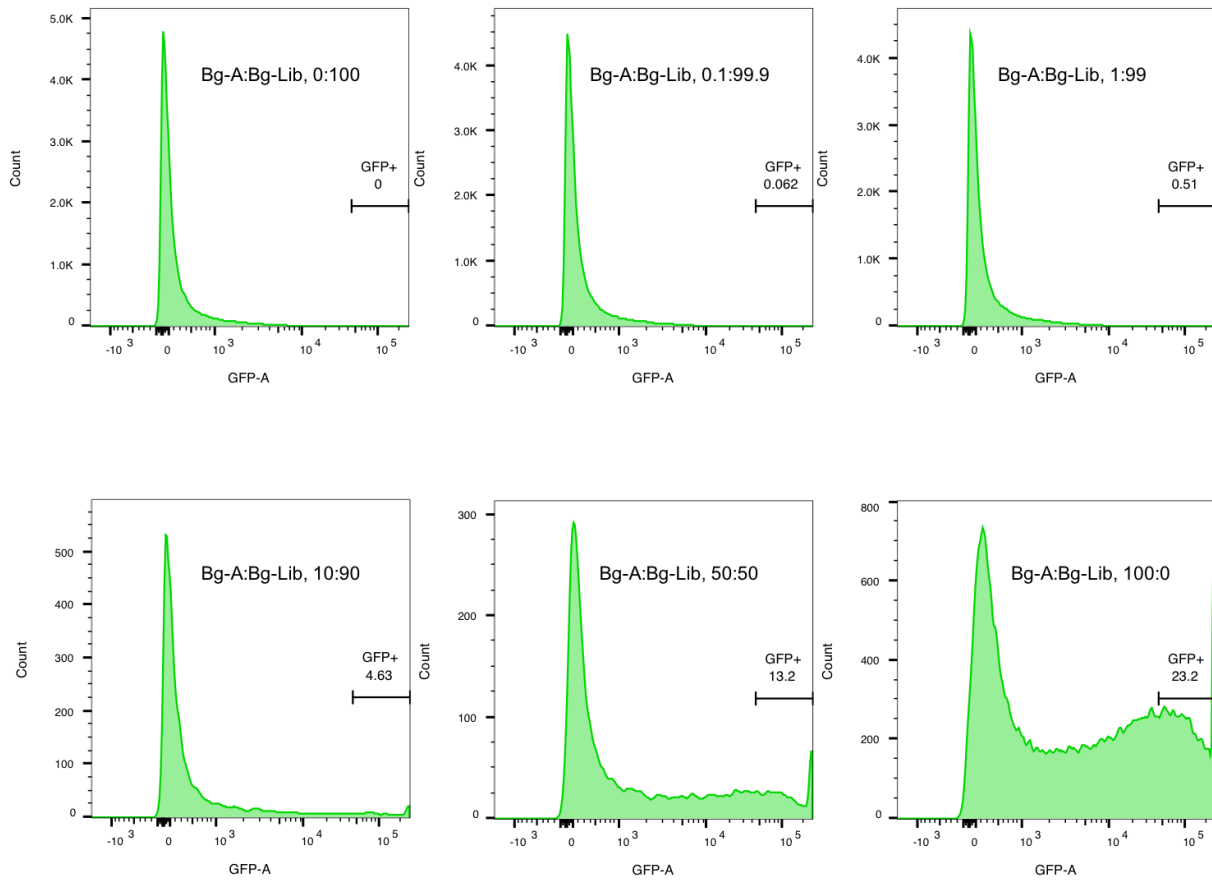
HEK293T, MB-MDA 231, and Caco2. The barcoded populations were co-transfected with each of the Recall plasmids (R-A, R-B, R-C) containing GFP + dCas9-VPR plasmid independently, causing instances of either match or mismatch with regards to the barcoded gRNA and Recall plasmid. GFP expression was measured 48 hours after transfection. Error load was quantified by comparatively tallying the values of the GFP-histogram, from high to low GFP intensity, of matching and mismatching recall samples. Specifically, sum totals of matching recall events were tabulated with respect to and along with each new accruing mismatch recall event. From these tabulations, % activation at a given error was calculated using the formula:

$$\frac{\sum \text{matching recall events at given error}}{\text{total matching events analyzed}}$$

% Error was calculated using the formula:  $\frac{\Sigma \text{ mismatching recall events}}{\Sigma \text{ matching recall events}}$ . The following data was charted onto a scatter plot and, using least squares fitting, generated exponential equations to model the data. (**Suppl Fig S4**). Fits for a vast majority of samples had an R<sup>2</sup> value of > 0.95. Experiments were performed in biological triplicate.



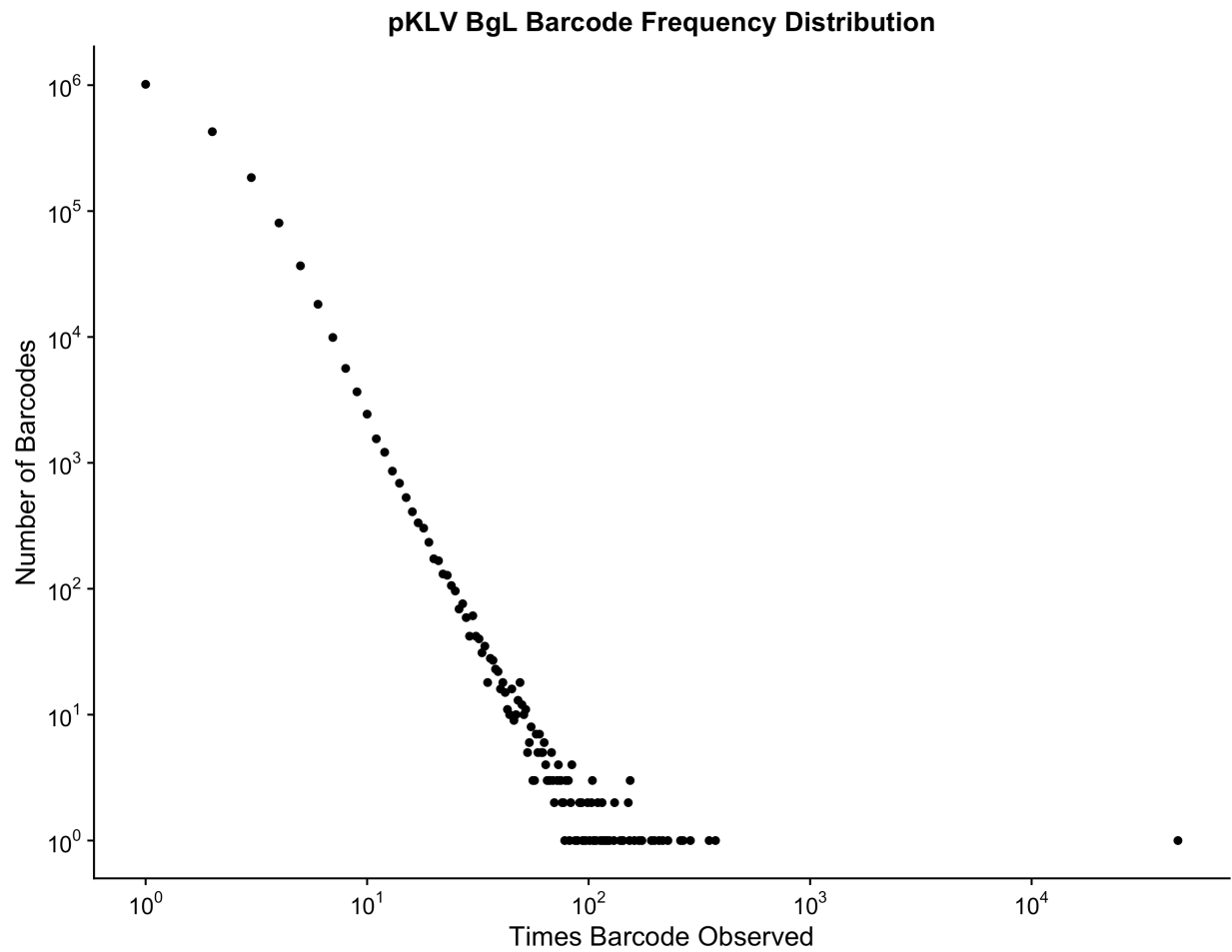
## Supplement Figure S5



### Supplementary Figure S5. HEK293T Bg-A/Bg-Library lineage dilution standard.

To initialize a standard and generate the gates for lineage isolation, a range of HEK293T Bg-A/Bg-library dilutions were plated in a 6 well plate: 0%Bg-A, 0.1%Bg-A, 1%Bg-A, 10%Bg-A, 50%Bg-A, and 100%Bg-A. The barcoded cell populations were co-transfected with Recall-A\_GFP and dCas9-VPR. Cells were analyzed via flow cytometry 48 hours post transfection. Sorting gates were set based off of the 0%Bg-A to both maximize capture of GFP positive cells while minimizing the capture noisy non-lineages of interest.

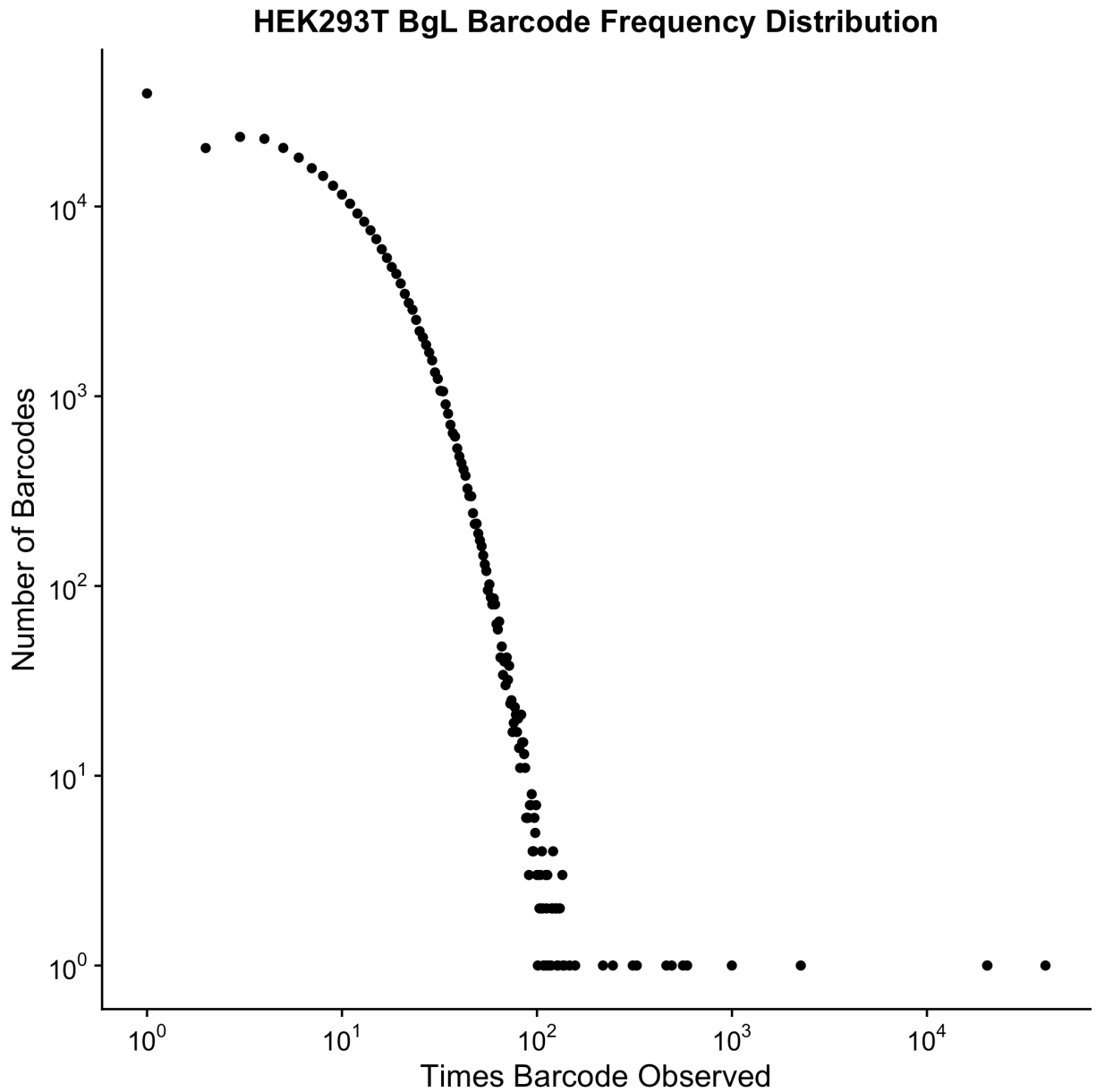
## Supplement Figure S6



### **Supplementary Figure S6. Barcode sampling of Lentiviral plasmid Bg-Library.**

Barcode sampling of plasmid DNA was performed to confirm the generation of a high diversity barcode-gRNA lentiviral transfer vector library. The barcodes were amplified from 50ng of the Lentiviral plasmid Bg-Library DNA and sequenced. This graph shows the barcode read frequency distribution of the library at a depth of  $4.1 \times 10^6$  reads. Barcode sampling revealed  $1.79 \times 10^6$  unique barcodes with >95% of the reads being represented by only 4 or fewer reads.

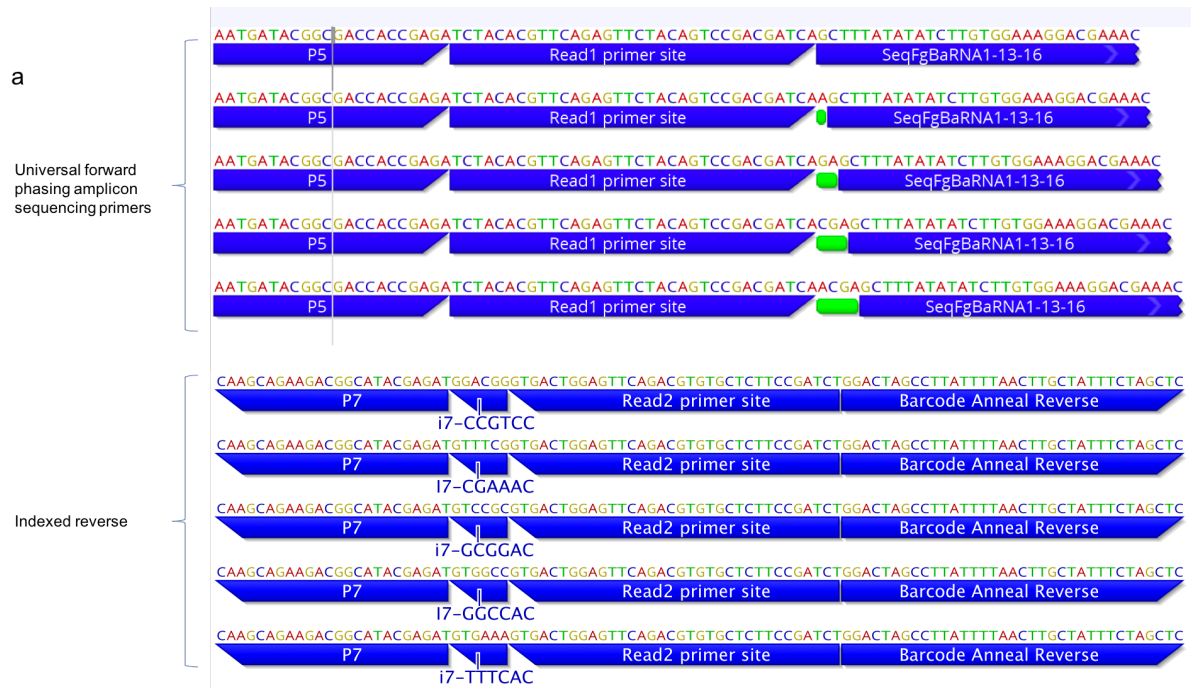
Supplement Figure S7



**Supplementary Figure S7. Barcode sampling of HEK293T Bg-Library.**

Barcode sampling of genomic DNA was performed to confirm the generation of a high diversity barcode-gRNA HEK293T library. The barcodes were amplified from 16 $\mu$ g of the HEK293T Bg-Library genomic DNA and sequenced. This graph shows the barcode read frequency distribution of the library at a depth of  $3.88 \times 10^6$  reads. Barcode sampling revealed  $3.01 \times 10^5$  unique barcodes.

**Supplement Figure S8**



**Supplementary Figure S8. Barcode amplification primers.**

**(a)** Annotated list of both forward and reverse amplification primers. The universal phasing amplicon forward primers and the indexed reverse primers contain both the flanking barcode annealing regions along with the relevant Illumina adaptor/indices, allowing for one-stage amplification of the genomically encoded barcoded gRNA. Utilization of the mixed universal forward phasing primers generates amplicons with staggered read 1 start sites, introducing necessary base diversity during Illumina sequencing of the barcoded amplicons. **(b)** Template of the amplified barcoded gRNA (not including the different phasing variants).

**Supplementary Figure S9. Lineage-specific BAX expression time-lapse imaging.**

Attached are movies that display lineage-specific activation of BAX and GFP in Caco-2 cells. Images were collected at 1 hour intervals for 24 hours of i) GFP only - R-A\_GFP ii) GFP and BAX - R-A\_BAX\_GFP and iii) GFP and BAX D71A - R-A BAX D71A\_GFP. In conditions that simultaneously express GFP and BAX, a signal delay is noted, showing GFP expression with subsequent Annexin V Red staining from BAX induced apoptosis. In the GFP and BAX D71A condition, the hyperactive BAX variant induces apoptosis significantly faster, resulting in contaminant Annexin V red and GFP signal onset.

**Filenames of Barcode match movies:**

Caco-2 phase\_red\_green\_Bg-A/R-A\_GFP  
Caco-2 phase\_red\_green\_Bg-A/R-A\_BAX\_GFP  
Caco-2 phase\_red\_green\_Bg-A/R-A BAX D71A\_GFP  
Caco-2\_red\_green\_Bg-A/R-A\_GFP  
Caco-2\_red\_green\_Bg-A/R-A\_BAX\_GFP  
Caco-2\_red\_green\_Bg-A/R-A BAX D71A\_GFP

**Filenames of Barcode mismatch movies:**

Caco-2 phase\_red\_green\_Bg-B/R-A\_GFP  
Caco-2 phase\_red\_green\_Bg-B/R-A\_BAX\_GFP  
Caco-2 phase\_red\_green\_Bg-B/R-A BAX D71A\_GFP  
Caco-2\_red\_green\_Bg-B/R-A\_GFP  
Caco-2\_red\_green\_Bg-B/R-A\_BAX\_GFP  
Caco-2\_red\_green\_Bg-B/R-A BAX D71A\_GFP